

Controlling the rotational and hyperfine state of ultracold $^{87}\text{Rb}^{133}\text{Cs}$ molecules

Philip D. Gregory,¹ Jesus Aldegunde,² Jeremy M. Hutson,^{3,*} and Simon L. Cornish^{1,†}

¹*Joint Quantum Centre (JQC) Durham-Newcastle, Department of Physics, Durham University, South Road, Durham DH1 3LE, United Kingdom*

²*Departamento de Química Física, Universidad de Salamanca, 37008 Salamanca, Spain*

³*Joint Quantum Centre (JQC) Durham-Newcastle, Department of Chemistry, Durham University, South Road, Durham DH1 3LE, United Kingdom*

(Received 10 August 2016; published 28 October 2016)

We demonstrate coherent control of the rotational and hyperfine state of ultracold, chemically stable $^{87}\text{Rb}^{133}\text{Cs}$ molecules with external microwave fields. We create a sample of ~ 2000 molecules in the lowest hyperfine level of the rovibronic ground state $N = 0$. We measure the transition frequencies to eight different hyperfine levels of the $N = 1$ state at two magnetic fields ~ 23 G apart. We determine accurate values of rotational and hyperfine coupling constants that agree well with previous calculations. We observe Rabi oscillations on each transition, allowing complete population transfer to a selected hyperfine level of $N = 1$. Subsequent application of a second microwave pulse allows the transfer of molecules back to a different hyperfine level of $N = 0$.

DOI: 10.1103/PhysRevA.94.041403

Ultracold heteronuclear molecules can provide many exciting new avenues of research in the fields of quantum-state-controlled chemistry [1,2], quantum information [3], quantum simulation [4,5], and precision measurement [6–8]. The large electric dipole moments accessible in such systems allow interactions to be tuned over length scales similar to the spacing between sites in an optical lattice. As such, this is an area of intense research with several groups recently reporting the production of dipolar molecules at ultracold temperatures [9–13].

Full control of the quantum state has been an invaluable tool in ultracold atom physics; it is therefore highly important to develop similar methods for ultracold molecules, addressing the complex rotational and hyperfine structures. Such control is at the heart of nearly all proposals for applications of ultracold polar molecules. For example, the rotational states of molecules might be used as pseudospins to simulate quantum magnetism [14,15]. This requires a coherent superposition of opposite-parity states to generate dipolar interactions [14], which may be probed by microwave spectroscopy [16,17]. Similarly, hyperfine states in the rotational ground state have been proposed as potential qubits for quantum computation [3,18,19]. In this context, robust coherent transfer between the hyperfine states is essential. Such transfer can be achieved using a scheme proposed by Aldegunde *et al.* [20] which employs microwave fields to manipulate the molecular hyperfine states. This approach has been implemented for the fermionic heteronuclear molecules $^{40}\text{K}^{87}\text{Rb}$ [21,22] and $^{23}\text{Na}^{40}\text{K}$ [23], leading to ground-breaking studies of the dipolar spin-exchange interaction [17] and nuclear-spin coherence time [19].

In this Rapid Communication, we report microwave spectroscopy of bosonic $^{87}\text{Rb}^{133}\text{Cs}$ in its ground vibrational state, and coherent state transfer from the absolute rovibrational and hyperfine ground state to a chosen single hyperfine state in either the first-excited or ground rotational states. We demonstrate the high precision with which we can map out the rotational energy structure of $^{87}\text{Rb}^{133}\text{Cs}$ in the lowest vibrational state. We use our measurements to obtain new values for the rotational constant, scalar spin-spin coupling constant, electric quadrupole coupling constants, and nuclear g factors (including shielding) for the molecule. Microwave π pulses are used to transfer the molecules first to a single hyperfine level of the first-excited rotational state, then back to a different hyperfine level of the rovibrational ground state.

We calculate the energy-level structure of $^{87}\text{Rb}^{133}\text{Cs}$ in the electronic and vibrational ground state by diagonalizing the Hamiltonian [24–27]

$$H = H_r + H_{\text{hf}} + H_Z, \quad (1)$$

where

$$H_r = B_v N^2 - D_v N^2 N^2, \quad (2a)$$

$$H_{\text{hf}} = \sum_{i=\text{Rb,Cs}} \mathbf{V}_i \cdot \mathbf{Q}_i + \sum_{i=\text{Rb,Cs}} c_i N \cdot \mathbf{I}_i + c_3 \mathbf{I}_{\text{Rb}} \cdot \mathbf{T} \cdot \mathbf{I}_{\text{Cs}} + c_4 \mathbf{I}_{\text{Rb}} \cdot \mathbf{I}_{\text{Cs}}, \quad (2b)$$

$$H_Z = -g_r \mu_N N \cdot \mathbf{B} - \sum_{i=\text{Rb,Cs}} g_i (1 - \sigma_i) \mu_N \mathbf{I}_i \cdot \mathbf{B}. \quad (2c)$$

The rotational contribution H_r [Eq. (2a)] is defined by the rotational angular momentum of the molecule N , and the rotational and centrifugal distortion constants B_v and D_v . The hyperfine contribution H_{hf} [Eq. (2b)] consists of four terms. The first describes the electric quadrupole interaction with coupling constants $(eqQ)_{\text{Rb}}$ and $(eqQ)_{\text{Cs}}$, while the second is the interaction between the nuclear magnetic moments and the magnetic field generated by the rotation of the molecule, with spin-rotation coupling constants c_{Rb} and c_{Cs} . The final two terms represent the tensor and scalar interactions between the nuclear magnetic moments, with tensor and scalar

*J.M.Hutson@durham.ac.uk

†S.L.Cornish@durham.ac.uk

Published by the American Physical Society under the terms of the Creative Commons Attribution 3.0 License. Further distribution of this work must maintain attribution to the author(s) and the published article's title, journal citation, and DOI.

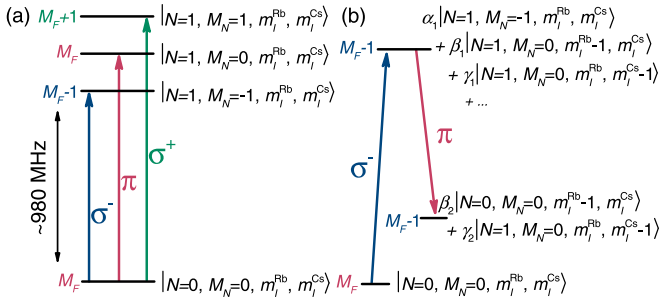


FIG. 1. (a) Electric dipole transitions between $N = 0$ and $N = 1$ rotational levels in the absence of hyperfine coupling. (b) Two-photon pulse sequence used to transfer population to a different hyperfine level of $N = 0$, taking advantage of mixing caused by hyperfine coupling.

spin-spin coupling constants c_3 and c_4 , respectively. Finally, the Zeeman contribution H_Z [Eq. (2c)] consists of two terms which represent the rotational and nuclear interaction with an externally applied magnetic field. The rotation of the molecule produces a magnetic moment which is characterized by the rotational g factor of the molecule (g_r). The nuclear interaction similarly depends on the nuclear g factors (g_{Rb} , g_{Cs}) and nuclear shielding (σ_{Rb} , σ_{Cs}) for each species. We do not apply electric fields in this work, which would require the addition of a further Stark contribution to the Hamiltonian and significantly complicate the spectra [28].

The nuclear spins in $^{87}\text{Rb}^{133}\text{Cs}$ are $I_{Rb} = \frac{3}{2}$ and $I_{Cs} = \frac{7}{2}$. At zero field, the total angular momentum $F = N + I_{Rb} + I_{Cs}$ is conserved. For the rotational ground state ($N = 0$), the total nuclear spin $I = I_{Rb} + I_{Cs}$ is very nearly conserved, and there are four hyperfine states with $I = 2, 3, 4,$ and 5 with separations determined by c_4 [27]. For excited rotational states, however, only F is conserved and I is a poor quantum number.

An external magnetic field splits each rotational manifold into $(2N + 1)(2I_{Rb} + 1)(2I_{Cs} + 1)$ Zeeman-hyperfine sublevels, so there are 32 levels for $N = 0$ and 96 levels for $N = 1$. Assignment of quantum numbers to the individual hyperfine levels is nontrivial and depends on the magnetic field regime [27]. The field mixes states with different values of F that share the same total projection M_F . At low fields, the levels are still approximately described by F and M_F (equivalent to I and M_I for $N = 0$). At high fields, however, the nuclear spins decouple and the individual projections M_N , m_I^{Rb} , and m_I^{Cs} become nearly good quantum numbers, with $M_F = M_N + m_I^{\text{Rb}} + m_I^{\text{Cs}}$.

A microwave field induces electric dipole transitions between rotational levels. At low fields, all transitions allowed by the selection rules $\Delta F = 0, \pm 1$ and $\Delta M_F = 0, \pm 1$ have significant intensity. At higher fields, however, additional selection rules emerge. If hyperfine couplings are neglected, electric dipole transitions leave the nuclear-spin states unchanged ($\Delta m_I^{\text{Rb}} = \Delta m_I^{\text{Cs}} = 0$) and are allowed only between neighboring rotational states such that $\Delta N = \pm 1$, $\Delta M_N = 0, \pm 1$ for microwave polarizations π, σ^\pm . In the absence of hyperfine interactions (where M_N would be a good quantum number) we would be able to drive at most three transitions from any given hyperfine level, as shown in Fig. 1(a).

Hyperfine coupling mixes states with different values of M_N , m_I^{Rb} , and m_I^{Cs} , and additional transitions become allowed. The couplings are principally due to scalar spin-spin coupling in $N = 0$ and nuclear quadrupole coupling in $N = 1$. The mixing allows us to use a multiphoton scheme to move the population to different hyperfine states of the rotational ground state. Figure 1(b) shows a simple example of this scheme, using two microwave photons to change the hyperfine state by $\Delta M_F = -1$.

Our experimental apparatus and method for creating ultracold $^{87}\text{Rb}^{133}\text{Cs}$ molecules have been discussed in previous publications [11,29–34]; we will therefore give only a brief overview here. We begin by using magnetoassociation on a magnetic Feshbach resonance to create weakly bound molecules from an ultracold atomic mixture confined in a crossed-beam optical trap ($\lambda = 1550$ nm) [33]. We remove the remaining atoms by means of the Stern-Gerlach effect, leaving a pure sample of trapped molecules. These molecules are then transferred to a single hyperfine state of the rovibrational ground state by stimulated Raman adiabatic passage (STIRAP) [11,35]. In this work, we create a sample of up to ~ 2000 $^{87}\text{Rb}^{133}\text{Cs}$ molecules in the lowest hyperfine state [shown in Fig. 2(a)] at a temperature of $1.17(1)$ μK and a peak density of $8.1(8) \times 10^{10} \text{ cm}^{-3}$. In order to measure the number of molecules in our experiment, we reverse both the STIRAP and magnetoassociation steps and subsequently use absorption imaging to detect the atoms that result from the molecular dissociation. Throughout, therefore, we always measure the number of molecules in the hyperfine state initially populated by STIRAP.

Our apparatus is equipped with two omnidirectional $\lambda/4$ antennas placed close to the outside of the fused silica cell. The polarization from each is roughly linear at the position of the molecules. They are oriented perpendicular to each other and aligned with respect to the static magnetic field such that one preferentially drives transitions with $\Delta M_F = 0$ and the other drives those with $\Delta M_F = \pm 1$. Each antenna is connected to a separate signal generator, which is frequency referenced to an external 10-MHz GPS reference. Fast (\sim ns) switches are used to generate microwave pulses of well-defined duration (typically 1–500 μs).

The large dipole moment of the molecule (1.225 D [11]) makes it easy to drive fast Rabi oscillations between neighboring rotational states. To perform the spectroscopy, therefore, we pulse on the microwave field for a time (t_{pulse}) which is less than the duration of a π pulse for the relevant transition ($< t_\pi$). We then observe the transition as an apparent loss of molecules as they are transferred into the first-excited rotational state. To avoid ac Stark shifts of the transition centers, the optical trap is switched off throughout the spectroscopy; the transition frequencies are thus measured in free space. We find that the widths of all of the features we measure are Fourier-transform limited, i.e., the width is proportional to $1/t_{\text{pulse}}$. We therefore iteratively reduce the power to get slower Rabi oscillations and allow longer pulse durations. Radically different t_{pulse} are required for different transitions, depending on the transition strength and antenna used. We carry out the spectroscopy at two different magnetic fields ~ 23 G apart; the field is calibrated using the microwave transition frequency between the $|f = 3, m_f = 3\rangle$ and $|f = 4, m_f = 4\rangle$ states of Cs.

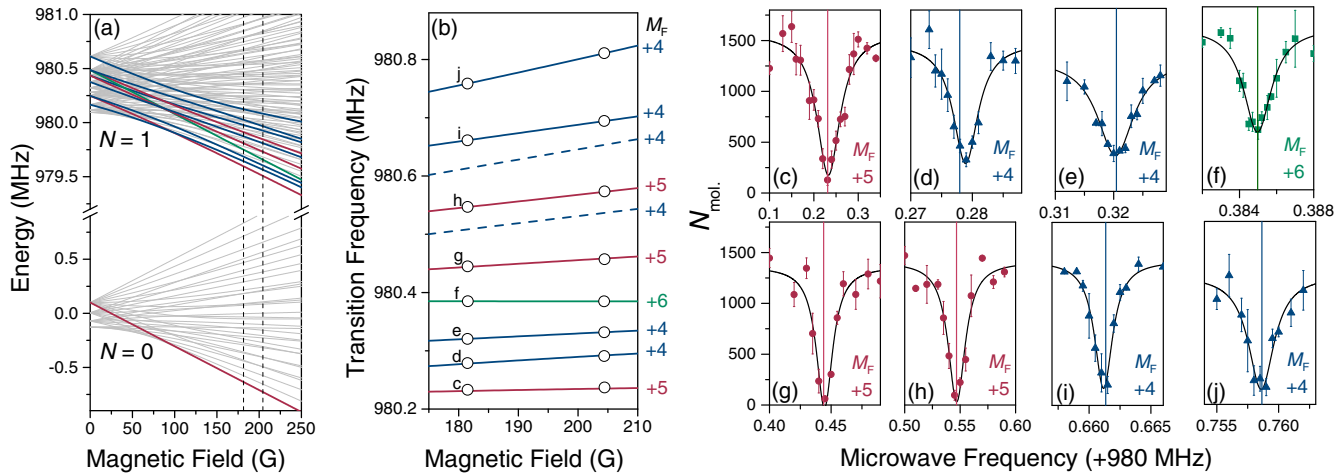


FIG. 2. Microwave spectroscopy of $^{87}\text{Rb}^{133}\text{Cs}$. (a) Hyperfine Zeeman structure of the $N=0$ and $N=1$ states. The $M_F=5$ initial state in $N=0$ is highlighted as a bold red line. The ten states in $N=1$ that are accessible from this initial state are shown as bold blue ($M_F=4$), red ($M_F=5$), and green ($M_F=6$) lines. The vertical dotted lines mark the two magnetic fields at which spectroscopy is performed in this work. (b) Comparison of experimentally measured transition frequencies from $|N=0, M_F=5\rangle$ to $|N=1, M_F=4, 5, 6\rangle$ with the fitted theory. Dashed lines indicate transitions that are weakly allowed but we have not observed. Error bars are not visible at this scale [36]. (c)–(j) Spectra of all the transitions found in this work at a magnetic field of ~ 181.5 G. The vertical lines show the transition frequencies given by the least-squares fit to obtain spectroscopic constants. The pulse durations used, chosen to be less than a π pulse for each transition, are (c) 12 μs , (d) 150 μs , (e) 100 μs , (f) 400 μs , (g) 60 μs , (h) 50 μs , (i) 400 μs , and (j) 200 μs .

With the population initially in the lowest hyperfine level ($M_F=5$) of the rovibrational ground state, we expect to find a maximum of ten transitions to the first-excited rotational state $|N=1, M_F=4, 5, 6\rangle$. We are able to observe eight of these transitions [36]. A complete set of spectra at a magnetic field of ~ 181.5 G is shown in Figs. 2(c)–2(j). Calculations of the expected intensities of the two unseen transitions show that the relative transition probability is $\sim 10^{-4}$ lower than for those we do observe.

We fit our model to the experimental spectra by minimizing the sum of the squared quotients between each residual and the uncertainty of the line. We fit the rotational constant, nuclear quadrupole constants, and scalar nuclear spin-spin constant. The nuclear g factors and shielding coefficients are multiplied together in the Hamiltonian so it is not possible to separate them, and we therefore fit the shielded g factors $g_{\text{Rb}}(1 - \sigma_{\text{Rb}})$ and $g_{\text{Cs}}(1 - \sigma_{\text{Cs}})$. The resulting values, along with the values of parameters held fixed at theoretical values, are given in Table I.

The fitted hyperfine parameters in Table I are all within 10% of the values predicted from DFT calculations [27], except for $(eQq)_{\text{Cs}}$, which is about 15% larger than calculated. This helps to calibrate the probable accuracy of the calculations for other alkali-metal dimers. The fitted value $c_4 = 19.0(1)$ kHz removes one of the two largest sources of error in our recent determination of the binding energy D_0 of $^{87}\text{Rb}^{133}\text{Cs}$ in its rovibrational ground state [38]; the zero-field hyperfine energy of the $M_F=5$ state is $(\frac{21}{4})c_4$, which increases from 90(30) kHz in Ref. [38] to 99.9(6) kHz. This increases the binding energy of the hyperfine-weighted vibronic bound state by 9 kHz, giving a revised value $D_0 = h \times 114\,268\,135.25(3)$ MHz. The fitted values of the shielded g factors $g_{\text{Rb}}(1 - \sigma_{\text{Rb}}) = 1.829(2)$ and $g_{\text{Cs}}(1 - \sigma_{\text{Cs}}) = 0.733(1)$ are consistent with the corresponding atomic values, 1.827 232(2) [39] and 0.732 357(1) [40] [with

the sign convention of Eq. (2c)]. The latter include shielding due to the electrons in the free atoms. Our values may be used in conjunction with the calculated molecular shielding factors ($\sigma_{\text{Rb}} = 3531$ ppm and $\sigma_{\text{Cs}} = 6367$ ppm [27]) to obtain values of the “bare” nuclear g factors 1.836(3) and 0.738(1).

The STIRAP transfer produces molecules in a spin-stretched state, where $|m_I^{\text{Rb}} + m_I^{\text{Cs}}|$ has its maximum possible

TABLE I. Constants involved in the molecular Hamiltonian for $^{87}\text{Rb}^{133}\text{Cs}$. Parameters not varied in the least-squares fit are taken from the literature. The majority of the fixed terms are calculated using density-functional theory (DFT) [27], with the exception of the centrifugal distortion constant D_v , which is obtained from laser-induced fluorescence combined with Fourier-transform spectroscopy (LIF-FTS) [37].

Constant	Value	Reference
B_v	490.155(5) MHz	[37]
	490.173 994(45) MHz	This work
D_v	213.0(3) Hz	[37]
	–872 kHz	[27]
$(eQq)_{\text{Rb}}$	–809.29(1.13) kHz	This work
$(eQq)_{\text{Cs}}$	51 kHz	[27]
	59.98(1.86) kHz	This work
c_{Rb}	29.4 Hz	[27]
c_{Cs}	196.8 Hz	[27]
c_3	192.4 Hz	[27]
c_4	17.3 kHz	[27]
	19.019(105) kHz	This work
g_{I}	0.0062	[27]
$g_{\text{Rb}}(1 - \sigma_{\text{Rb}})$	1.8295(24)	This work
$g_{\text{Cs}}(1 - \sigma_{\text{Cs}})$	0.7331(12)	This work

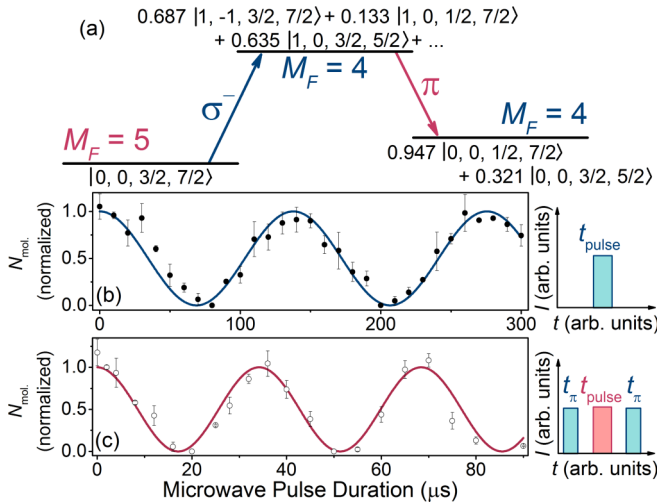


FIG. 3. Coherent population transfer of molecules between specific hyperfine states in rotational levels $N = 0$ and $N = 1$. (a) Transfer scheme followed in this work. All molecules start in the lowest hyperfine state ($M_F = 5$) of $N = 0$. States are described in the uncoupled basis set $|N, M_N, m_I^{\text{Rb}}, m_I^{\text{Cs}}\rangle$. (b) Rabi oscillations in one-photon transfer of molecules to the single hyperfine level of $N = 1$ shown in (a). (c) Rabi oscillations in two-photon transfer, using a π pulse on the first transition and a second microwave pulse with different frequency and polarization to drive transitions to the $M_F = 4$ hyperfine state of $N = 0$ shown in (a).

value and $M_N, m_I^{\text{Rb}}, m_I^{\text{Cs}}$ are all good quantum numbers. However, the other hyperfine states of both $N = 0$ and 1 are significantly mixed in the uncoupled basis set at the fields considered here, and have no good quantum numbers other than M_F . In Fig. 3, we demonstrate complete transfer of the molecular population between these mixed-character hyperfine states. We begin by transferring the molecules to an $M_F = 4$ level of $N = 1$ [transition frequency of 980 320.47 kHz, shown in Fig. 2(e)]. The eigenvector component of the uncoupled basis function that couples to our initial $N = 0$ hyperfine level is ~ 0.687 . With the microwave power available, π pulses on this transition can be driven with pulse durations $< 10 \mu\text{s}$, though it is important when using short pulses that the separation between available states is greater than the Fourier width of the pulse. We reduce

the microwave power such that the Rabi frequency of the transition is $\Omega_{\sigma^-}/2\pi = 7.26(5)$ kHz, as shown in Fig. 3(b), ensuring that we do not couple to neighboring transitions. Single π pulses allow complete transfer of the population to the destination hyperfine level. We subsequently transfer the molecules to a different hyperfine level of $N = 0$ by applying a second microwave field with a different polarization and frequency. We choose to use π -polarized microwaves to transfer the molecules to the higher energy of the two $M_F = 4$ levels of $N = 0$ (transition frequency of 980 119.14 kHz). At this field, the composition of this final level is $0.947 |0, 0, \frac{1}{2}, \frac{7}{2}\rangle + 0.321 |0, 0, \frac{3}{2}, \frac{5}{2}\rangle$ in the uncoupled basis $|N, M_N, m_I^{\text{Rb}}, m_I^{\text{Cs}}\rangle$. We observe Rabi oscillations on the second transition by pulsing on the π -polarized microwaves between two π pulses on the σ^- -polarized microwave transition, as shown in Fig. 3(c). Coherent transfer is achieved with a Rabi frequency of $\Omega_{\pi}/2\pi = 29.2(3)$ kHz.

In summary, we have performed high-precision microwave spectroscopy of ultracold $^{87}\text{Rb}^{133}\text{Cs}$ molecules in the vibrational ground state, and have accurately determined the hyperfine coupling constants for the molecule. Our results confirm that the hyperfine coupling constants calculated by Aldegunde *et al.* [27] are generally accurate to within $\pm 10\%$, calibrating the probable accuracy of the calculations for other alkali-metal dimers. The resulting understanding of the hyperfine structure enables full control of the quantum state, and we have demonstrated coherent transfer to a chosen hyperfine state in either the first-excited or ground rotational state. Such complete control is essential for many proposed applications of ultracold polar molecules, and opens the door to a range of exciting future experimental directions, including studies of quantum magnetism [14,15] and novel many-body phenomena [5,41].

This work was supported by the U.K. Engineering and Physical Sciences Research Council (EPSRC) Grants No. EP/H003363/1, No. EP/I012044/1, No. and GR/S78339/01. J.A. acknowledges funding by the Spanish Ministry of Science and Innovation Grants No. CTQ2012-37404-C02 and No. CTQ2015-65033-P, and Consolider Ingenio 2010 CSD2009-00038.

The data presented in this paper are available at DOI:10.15128/R12J62S485J.

- [1] S. Ospelkaus, K.-K. Ni, D. Wang, M. H. G. de Miranda, B. Neyenhuis, G. Quémener, P. S. Julienne, J. L. Bohn, D. S. Jin, and J. Ye, *Science* **327**, 853 (2010).
- [2] R. V. Krems, *Phys. Chem. Chem. Phys.* **10**, 4079 (2008).
- [3] D. DeMille, *Phys. Rev. Lett.* **88**, 067901 (2002).
- [4] L. Santos, G. V. Shlyapnikov, P. Zoller, and M. Lewenstein, *Phys. Rev. Lett.* **85**, 1791 (2000).
- [5] M. A. Baranov, M. Dalmonte, G. Pupillo, and P. Zoller, *Chem. Rev.* **112**, 5012 (2012).
- [6] V. V. Flambaum and M. G. Kozlov, *Phys. Rev. Lett.* **99**, 150801 (2007).
- [7] T. A. Isaev, S. Hoekstra, and R. Berger, *Phys. Rev. A* **82**, 052521 (2010).
- [8] J. J. Hudson, D. M. Kara, I. J. Smallman, B. E. Sauer, M. R. Tarbutt, and E. A. Hinds, *Nature (London)* **473**, 493 (2011).
- [9] K.-K. Ni, S. Ospelkaus, M. H. G. de Miranda, A. Pe'er, B. Neyenhuis, J. J. Zirbel, S. Kotochigova, P. S. Julienne, D. S. Jin, and J. Ye, *Science* **322**, 231 (2008).
- [10] T. Takekoshi, L. Reichsöllner, A. Schindewolf, J. M. Hutson, C. R. Le Sueur, O. Dulieu, F. Ferlaino, R. Grimm, and H.-C. Nägerl, *Phys. Rev. Lett.* **113**, 205301 (2014).
- [11] P. K. Molony, P. D. Gregory, Z. Ji, B. Lu, M. P. Köppinger, C. R. Le Sueur, C. L. Blackley, J. M. Hutson, and S. L. Cornish, *Phys. Rev. Lett.* **113**, 255301 (2014).
- [12] J. W. Park, S. A. Will, and M. W. Zwierlein, *Phys. Rev. Lett.* **114**, 205302 (2015).

- [13] M. Guo, B. Zhu, B. Lu, X. Ye, F. Wang, R. Vexiau, N. Bouloufa-Maafa, G. Quéméner, O. Dulieu, and D. Wang, *Phys. Rev. Lett.* **116**, 205303 (2016).
- [14] R. Barnett, D. Petrov, M. Lukin, and E. Demler, *Phys. Rev. Lett.* **96**, 190401 (2006).
- [15] A. V. Gorshkov, S. R. Manmana, G. Chen, J. Ye, E. Demler, M. D. Lukin, and A. M. Rey, *Phys. Rev. Lett.* **107**, 115301 (2011).
- [16] K. R. A. Hazzard, A. V. Gorshkov, and A. M. Rey, *Phys. Rev. A* **84**, 033608 (2011).
- [17] B. Yan, S. A. Moses, B. Gadway, J. P. Covey, K. R. A. Hazzard, A. M. Rey, D. S. Jin, and J. Ye, *Nature (London)* **501**, 521 (2013).
- [18] A. André, D. DeMille, J. M. Doyle, M. D. Lukin, S. E. Maxwell, P. Rabl, R. J. Schoelkopf, and P. Zoller, *Nat. Phys.* **2**, 636 (2006).
- [19] J. W. Park, Z. Z. Yan, H. Loh, S. A. Will, and M. W. Zwiwerlein, [arXiv:1606.04184](https://arxiv.org/abs/1606.04184).
- [20] J. Aldegunde, H. Ran, and J. M. Hutson, *Phys. Rev. A* **80**, 043410 (2009).
- [21] S. Ospelkaus, K.-K. Ni, G. Quéméner, B. Neyenhuis, D. Wang, M. H. G. de Miranda, J. L. Bohn, J. Ye, and D. S. Jin, *Phys. Rev. Lett.* **104**, 030402 (2010).
- [22] B. Neyenhuis, B. Yan, S. A. Moses, J. P. Covey, A. Chotia, A. Petrov, S. Kotochigova, J. Ye, and D. S. Jin, *Phys. Rev. Lett.* **109**, 230403 (2012).
- [23] S. A. Will, J. W. Park, Z. Z. Yan, H. Loh, and M. W. Zwiwerlein, *Phys. Rev. Lett.* **116**, 225306 (2016).
- [24] N. F. Ramsay, *Phys. Rev.* **85**, 60 (1952).
- [25] J. M. Brown and A. Carrington, *Rotational Spectroscopy of Diatomic Molecules* (Cambridge University Press, Cambridge, U.K., 2003).
- [26] D. L. Bryce and R. E. Wasylshen, *Acc. Chem. Res.* **36**, 327 (2003).
- [27] J. Aldegunde, B. A. Rivington, P. S. Żuchowski, and J. M. Hutson, *Phys. Rev. A* **78**, 033434 (2008).
- [28] H. Ran, J. Aldegunde, and J. M. Hutson, *New J. Phys.* **12**, 043015 (2010).
- [29] M. L. Harris, P. Tierney, and S. L. Cornish, *J. Phys. B* **41**, 059803 (2008).
- [30] D. L. Jenkin, D. J. McCarron, M. P. Köppinger, H. W. Cho, S. A. Hopkins, and S. L. Cornish, *Eur. Phys. J. D* **65**, 11 (2011).
- [31] H. W. Cho, D. J. McCarron, D. L. Jenkin, M. P. Köppinger, and S. L. Cornish, *Eur. Phys. J. D* **65**, 125 (2011).
- [32] D. J. McCarron, H. W. Cho, D. L. Jenkin, M. P. Köppinger, and S. L. Cornish, *Phys. Rev. A* **84**, 011603 (2011).
- [33] M. P. Köppinger, D. J. McCarron, D. L. Jenkin, P. K. Molony, H. W. Cho, S. L. Cornish, C. R. Le Sueur, C. L. Blackley, and J. M. Hutson, *Phys. Rev. A* **89**, 033604 (2014).
- [34] P. D. Gregory, P. K. Molony, M. P. Köppinger, A. Kumar, Z. Ji, B. Lu, A. L. Marchant, and S. L. Cornish, *New J. Phys.* **17**, 055006 (2015).
- [35] P. K. Molony, P. D. Gregory, A. Kumar, C. R. Le Sueur, J. M. Hutson, and S. L. Cornish, *ChemPhysChem* (2016).
- [36] See Supplemental Material at <http://link.aps.org/supplemental/10.1103/PhysRevA.94.041403> for both the experimental center frequencies for all eight transitions at both magnetic fields used, together with frequencies calculated with the fitted values of the molecular constants.
- [37] C. E. Fellows, R. F. Gutterres, A. P. C. Campos, J. Vergès, and C. Amiot, *J. Mol. Spectrosc.* **197**, 19 (1999).
- [38] P. K. Molony, A. Kumar, P. D. Gregory, R. Kliese, T. Puppe, C. R. Le Sueur, J. Aldegunde, J. M. Hutson, and S. L. Cornish, *Phys. Rev. A* **94**, 022507 (2016).
- [39] C. W. White, W. M. Hughes, G. S. Hayne, and H. G. Robinson, *Phys. Rev.* **174**, 23 (1968).
- [40] C. W. White, W. M. Hughes, G. S. Hayne, and H. G. Robinson, *Phys. Rev. A* **7**, 1178 (1973).
- [41] L. D. Carr, D. DeMille, R. V. Krems, and J. Ye, *New J. Phys.* **11**, 055049 (2009).